Performance of lignin derived compounds as octane boosters

Miao Tian, Robert L Mccormick, Matthew A Ratcliff, Jon Luecke, Janet Yanowitz, Pierre-Alexandre Glaude, Michel Cuijpers, Michael D Boot

Performance of Lignin Derived Compounds as Octane Boosters

Miao Tian

Technical University of Eindhoven, P.O. Box 513, 5600 MB, Eindhoven, Netherlands. Fax:+31(0)40 247 2140; Tel:+31(0)40 247 2877

Robert L. McCormick

National Renewable Energy Laboratory, Golden, Colorado 80401, United States.

Matthew A. Ratcliff

National Renewable Energy Laboratory, Golden, Colorado 80401, United States.

Jon Luecke

National Renewable Energy Laboratory, Golden, Colorado 80401, United States.

Janet Yanowitz

EcoEngineering, Inc., Boulder, Colorado 80304, United States.

Pierre-Alexandre Glaude

Laboratoire Réactions et Génie des Procédés (LRGP), CNRS, Université de Lorraine, ENSIC, 1 rue Grandville, 54000 Nancy, France

Michel Cuijpers

Technical University of Eindhoven, P.O. Box 513, 5600 MB, Eindhoven, Netherlands.

Michael D. Boot

Technical University of Eindhoven, P.O. Box 513, 5600 MB, Eindhoven, Netherlands.

Email addresses: m.tian@tue.nl (Miao Tian), Robert.McCormick@nrel.gov (Robert L. McCormick), Matthew.Ratcliff@nrel.gov (Matthew A. Ratcliff), Jon.Luecke@nrel.gov (Jon Luecke), ecoeng.yano@gmail.com (Janet Yanowitz), pierre-alexandre.glaude@univ-lorraine.fr (Pierre-Alexandre Glaude), M.C.M.Cuijpers@tue.nl (Michel Cuijpers), m.d.boot@tue.nl (Michael D. Boot)

Abstract

The performance of spark ignition engines is highly dependent on fuel anti-knock quality, which in turn is governed by autoignition chemistry. In this study, we explore this chemistry for various aromatic oxygenates (i.e., anisole, 4-methyl anisole, 4-propyl anisole, guaiacol, 4-methyl guaiacol, 4-ethyl guaiacol) that can be produced from lignin, a low value residual biomass stream that is generated in paper pulping and cellulosic ethanol plants. All compounds share the same benzene ring, but have distinct oxygen functionalities and degrees of alkylation. The objective of this study is to ascertain what the impact is of said side groups on anti-knock quality and, by proxy, on fuel economy in a modern Volvo T5 spark ignition engine. To better comprehend the variation in behavior amongst the fuels, further experiments have been conducted in a constant volume autoignition device. The results demonstrate that alkylation has a negligible impact on anti-knock quality, while the addition of functional oxygen groups manifests as a deterioration in anti-knock quality.

Keywords: Lignin, knock, constant volume autoignition, anisole, guaiacol, octane boosters

---

1. Introduction

1.1. Requirements

At present, the most widely adopted strategy to further improve the efficiency of spark ignition (SI) engine is a combination of downsizing and turbocharging. The associated higher engine loads, however, increase the risk of knock [1] and therefore can be pursued more aggressively with more knock resistant fuels.

Knock resistance has been conventionally quantified in terms of the research octane number (RON) and the motor octane number (MON). RON is measured at lower speed and temperature conditions relative to MON. The two tests thus represent distinct engine operating regimes. An attempt to create a more generic measure for anti-knock quality, Kalghatgi [2] proposed the concept of octane index (OI):

$$OI = (1-K)\cdot RON + K\cdot MON = RON - K\cdot(RON - MON) = RON - K\cdot S \quad (1)$$

In this equation, S denotes the so-called octane sensitivity of a fuel's auto-ignition chemistry to temperature. Mathematically, S is the difference between RON and MON.

When $K = 0$ and $K = 1$, the OI is by definition equal to RON and MON, respectively. The constant K is a function of unburnt gas (end gas) temperature and pressure and is a property of the engine, not the fuel. A number of studies show that over time K values have on average become lower, consistent with better intake air and cylinder cooling, as well as more efficient combustion processes which reject less chemical energy as heat [1, 3–5]. Negative K values have been reported for downsized, turbocharged engines, which in practice implies that knock resistance as measured by the OI is greater than RON for those fuels having a octane sensitivity greater than zero [3–5].

Aromatics are among the highest RON and S compounds found in gasoline today. The past decades, however, have seen legislation come into force that curbs aromatic levels in gasoline, citing concerns regarding toxicity. In the EU, aromatic content is currently limited to maximum 35% [6].

Omission of aromatics from the mix means that other high octane and S com-

ponents must be used to maintain a target level of knock resistance. For high RON this can be achieved by blending paraffinic compounds such as iso-octane, which has a RON of 100. While solving the RON issue, iso-octane has by definition an *S* of 0 and thus cannot elevate this value back into pre-aromatic legislation territory. There are nevertheless other octane boosters on the market that do possess both aforementioned attributes, such as ethyl-tert-butylether (ETBE) and ethanol [1, 6, 7].

1.2. Market premium

Starting from any feedstock, it makes sound economic sense to aim production processes towards compounds that have good anti-knock quality. The case for this becomes quite clear when reviewing the data in Table 1. Evidently, an average market premium of 5-22.5 US$/ton (Table 1, far right column) can be commanded for every RON point in excess of the 95 European benchmark.

When not crude oil but biomass is considered as the feedstock of choice, the case for producing octane boosters is even more pronounced. Biofuels typically contain oxygen in their molecular structure. This oxygen is often argued to be commercially detrimental, owing to the associated reduction in (lower) heating value (Table 1, 2nd column). In the event a biofuel can be marketed as an octane booster, however, the prevailing price becomes decoupled from the *sec* calorific value (Table 1, 4th and 5th columns).

Combined high RON and *S* values have been reported for various aromatic oxygenates that might in future be produced from lignin, a residual stream produced and burnt to generate heat and steam in paper pulping and cellulosic ethanol plants [9]. Table 2 shows some of the aromatic (oxygenates) or aromatic blend-

Table 1: European spot market prices for RON95 gasoline and various octane boosters

Fuel	LHV [MJ/kg]	RON	premium [8] [$/ton]	premium [$/GJ]	premium [a] [$/ton+/RON+]	premium [$/Gal+/RON+][b]
Gasoline	41.9	95	500.75	11.95	0	0
Ethanol[c]	27	109	816.5	30.3	22.5	0.074
MTBE	35.1	117	610.92	17.4	5.0	0.014
ETBE	36.3	119	692	18.9	8.0	0.021

[a] The premium of other fuels compared to gasoline per ton per RON, e.g. for MTBE, (610.92-500.75)/(117-95)=5

[b] US gallon

[c] The spot price of ethanol in the US (American CBOT), as of June 19 2016, is 1.66 $/gallon or roughly 555.8 $/ton. This translates into a RON premium of 3.90 $/ton+/RON+, 0.018 $/Gal+/RON+.

ings from literature, which have high RON and S. From a review of earlier data on DCN for various aromatic oxygenates [10], it becomes clear that DCN increases proportionally with the number of functional oxygen groups, irrespective of group type or whether or not the ring is alkylated with C1-C3 chains (Figure 1).

While there have been many studies on the performance of lignin derived aromatic oxygenates in compression ignition engines [13–18], little is known about their potential as renewable octane boosters. The goal of this paper is to determine both qualitatively and quantitatively the anti-knock quality of various members of two important families of aromatic oxygenates - anisoles and guaiacols - that are frequently subject of discussion in lignin related literature. Anti-knock quality

Table 2: Octane number of some aromatic (oxygenates)

	RON	MON	S
P-xylene [11]	116.4	109	7.4
Ethylbenzene [11]	107	97.5	9.5
2-Phenyl ethanol [12]	110	90	20
10 vol-% Benzyl alcohol with Euro95 [9]	96.9	86.6	10.3
10 vol-% Acetophenone with Euro95 [9]	96.1	86.6	9.5

is evaluated in a port-fuel injected turbo-charged SI engine and ignition quality tester (IQT). Distinctions found amongst the fuels are subsequently explained by means of kinetic model.

2. Aromatic oxygenates

Lignin, a critical component of plant cell walls, is the third most abundant natural polymer after cellulose and hemi-cellulose. Its large quantity and chemical structure make it an attractive feedstock for producing bio-aromatics [19]. As a three-dimensional amorphous polymer consisting of methoxylated phenylpropane structures, including mono-, di-, and poly-alkyl substituted phenols, benzenes and alkyoxybenzenes, connected by C-O-C and C-C bonds [20], it is the largest direct source of aromatics found in nature.

There are three principal types of monolignols, or monomer units in lignin, namely p-coumaryl, coniferyl alcohol and sinapyl alcohol [21] (Figure 2).

Given that a wide variety of compounds can be produced from these units, a survey of the lignin literature has been conducted to reveal the most prevalent aro-

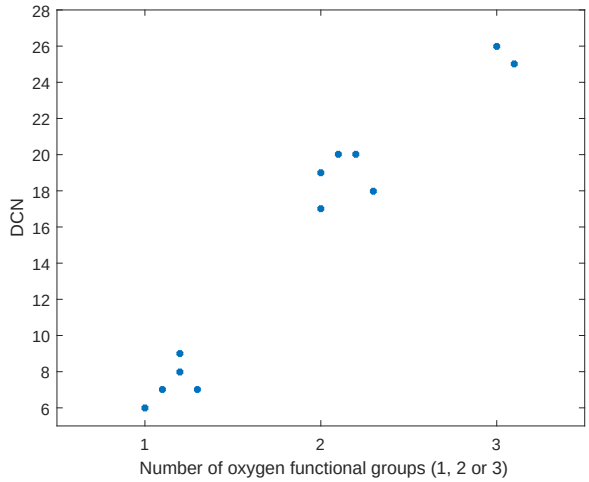

Figure 1: DCN as a function of number of functional oxygen groups for various types of oxygenated aromatics. Underlying data retrieved from [10]

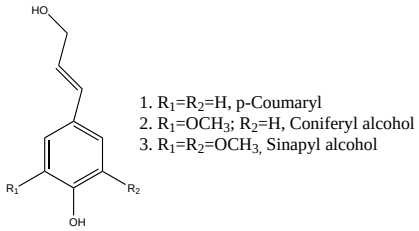

Figure 2: Lignin monolignols [22]

matic oxygenates that are also liquid at room temperature. Listed in Table 3, these are anisole and guaiacol, as well as the most common alkylated versions thereof, namely 4-methyl anisole (4-MA), 4-propyl anisole (4-PA), 4-methyl guaiacol (4-MG) and 4-ethyl guaiacol (4-EG). This set of compounds will allow us to analyze the impact of both alkylation and functional oxygen groups on anti-knock quality.

Table 3: Aromatic oxygenates frequently cited in lignin studies

Compound	References
anisole	[10, 23–29]
4-MA	[10, 26, 28–32]
4-PA	[10, 29, 33]
guaiacol	[10, 23, 24, 26, 34–50]
4-MG	[10, 32, 38, 39, 42, 43, 45, 49–53]
4-EG	[10, 25, 32, 39, 42, 43, 45, 51–56]

3. Methodology

3.1. Fuel matrix

3.1.1. Base fuel

Detailed hydrocarbon analysis of the Euro95 base fuel has been conducted in accordance with ASTM method D6729 [57] (Table 4). The results indicate that this commercial gasoline used in the Netherlands has a relatively high aromatic content, notably toluene (14-vol%). The following oxygenates were also identified in the base fuel: methanol, ethanol and MTBE at 0.4%, 3.9%, 3.1% by volume, respectively.

3.1.2. Oxygenates

The molecular structures of the oxygenated aromatics investigated in this study are shown in Figure 3. Associated physiochemical properties are tabulated in Table 5.

Measurement of octane numbers for pure components with high boiling points

Table 4: Components of Euro95

Component	vol.-%
Paraffin	48.90
Aromatics	31.58
Olefins	6.62
Oxygentates	7.44
Naphthenes	4.60
Others	0.86
Average molecular weight	87.53
Empirical formula	$C_{6.11}H_{11.51}O_{0.12}$

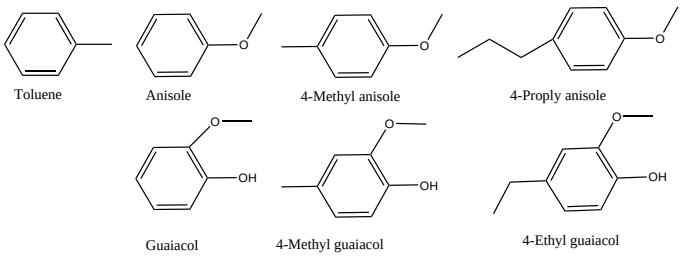

Figure 3: Molecular structures of selected aromatic oxygenates

Table 5: Physiochemical properties of neat compounds

Fuel	Formula	Density g/L	BP[a] °C	Viscosity[b] cP	LHV[c] MJ/L	DCN[c]	RON	MON
Toluene	C_7H_8	0.865	110	0.557	35.27	3	116[d]	102[d]
Anisole	C_7H_8O	0.995	154	1.00	33.19	6.4	103[e]	92[e]
4-MA	$C_8H_{10}O$	0.941	174	1.08	33.38	7.4	104[e]	92[e]
4-PA	$C_{10}H_{14}O$	0.941	215	1.64	34.22	7.5	–	–
Guaiacol	$C_7H_8O_2$	1.129	205	6.01	31.06	19.3	–	–
4-MG	$C_8H_{10}O_2$	1.092	221	7.70	31.57	19.8	–	–
4-EG	$C_9H_{12}O_2$	1.063	234	6.50	30.48	19.6	–	–

[a] Boiling point

[b] @ 25°C.

[c] Toluene [58]; aromatic oxygenates [10]

[d] [59]

[e] ASTM method D2699 (RON) and D2700 (MON)

is challenging and was not attempted in this study. However, derived cetane number (DCN) is a measure of autoignition tendency that is inversely proportional to octane number but is easily measured for pure compounds with high boiling points [58]. Therefore, DCNs from McCormick et al. [10] were used (Table 5). A further observation is that the boiling points of 4-PA, guaiacol, 4-MG and 4-EG are relatively high in comparison to the ASTM D4814, distillation temperature T90 and final boiling point limits of 190 and 225°C, respectively.

3.1.3. Blends

Compared to the RON95 base fuel (Euro95), all blends with 10 vol-% aromatic oxygenates yield a similar or modestly higher volumetric LHV, an elevated oxygen content notwithstanding (Table 6). The RON and MON of Euro 95, anisole and guaicol blends were measured, anisole blend shows higher RON than Euro95, while guaiacol blend has same RON and slightly less MON.

Table 6: Properties of fuel blends

Fuel	Density g/L	O content [wt.-%]	LHV[a] MJ/kg	LHV[a] MJ/L	Viscosity[b] cP	RON	MON
Euro 95	0.74	2.24	41.91	31.01	0.31	95.0[c]	85.6[c]
10% Toluene	0.756	2.02	41.78	31.58	0.38	–	–
10% Anisole	0.764	3.46	40.79	31.15	0.33	97.4[c]	86.8[c]
10% 4-MA	0.766	3.26	40.96	31.37	0.35	–	–
10% 4-PA	0.764	3.00	41.22	31.51	0.35	–	–
10% Guaiacol	0.785	4.86	39.82	31.24	0.37	95.0[c]	84.1[c]
10% 4-MG	0.778	4.49	40.07	31.18	0.40	–	–
10% 4-EG	0.777	4.20	40.08	31.15	0.40	–	–

[a] Values computed with molar blending rule

[b] Blend viscosity were calculated using the Refutas equation [60]

[c] Measured using ASTM method D2699 (RON) and D2700 (MON) by ASG Analytik-Service Gesellschaft mbH

3.2. Engine experiments

A 2.5L 5-cylinder Volvo T5 port-fuel injected turbocharged gasoline engine was used in this study (Table 7). The test rig is equipped with a water-cooled Schenck E2330 eddy current brake. A Kistler piezoelectric pressure sensor with a resolution of 3600 samples per crank shaft rotation has been installed into one of the cylinders for pressure analysis.

Table 7: Engine specifications

Engine	2.5T (B5254T6)
Type	In-line 5-cylinder LPT
Displacement [cm3]	2521
Bore [mm]	83
Stroke [mm]	93.2
Combustion chamber type	Pent-roof
Compression ratio [-]	9.0:1
Valves per cylinder	4
Ignition sequence	1-2-4-5-3
Fuel, octane requirement [RON]	95-98
Max. output [kW(HP)@RPM]	147(200)@4800
Max. torque [Nm@RPM]	300@1500-4500
Max. boost pressure [bar]	1.38

Engine experiments were conducted at stoichiometric conditions, wide open throttle (WOT) and low speed (1500 RPM). Spark timing was advanced until the onset of knock, the definition of which will be presented later on. The spark tim-

ing and boost pressure used for the baseline gasoline measurements was 12 crank angle degrees before top dead center (°CA bTDC) and 1.26 bar, respectively. Intake air temperature was regulated by means of an external heat exchanger and kept constant at roughly 20°C. Engine-out coolant and oil temperatures were kept constant at approximately 91°C. All remaining engine settings were kept at their stock values.

Knock intensity (KI) was quantified by means of the maximum amplitude pressure - peak-to-peak - oscillation (MAPO) method [61]. The MAPO value is obtained by filtering the in-cylinder pressure profile with a 6-25 kHz bandpass filter. The knock threshold is met when the knock intensity (KI), as expressed by MAPO, equals 0.25 bar. The spark timing at which this event occurs is referred to as the knock limited spark advance (KLSA). Besides cycle-by-cycle variation, the engine experiments will also vary day to day, so the day-to-day variation of the base gasoline was recorded during the measurement (four different days), the standard deviation of these measurement are shown as error bars in the engine performance results. Limited by the amount of fuels purchased, the other fuels have only tested in one day, so no day-to-day variation shows here.

3.3. Constant volume autoignition experiments

A modified ignition quality tester (IQT) was used to study the temperature dependency of autoignition for the oxygenates. The IQT is a constant volume combustion chamber, equipped with a fuel injection system in accordance with the ASTM method D6890 for measuring DCN [62]. ID is defined here as the duration between the start of injection and the time at which the pressure reaches the so-called pressure recovery point of 138 kPa above the value prior to fuel

injection.

However, the ASTM D6890 method is known to produce a heterogeneous fuel-air mixture such that the ignition delay time measured is a combination of physical and chemical kinetic factors. Bogin et al. have modified the IQT controls and operating parameters for use in more fundamental ignition delay and kinetic mechanism validation studies [63–65]. The authors observed that for a sufficiently long auto-ignition delay time (ID) (e.g., $>$ 40 ms), the mixture conditions are nearly homogeneous in nature. In such an environment, chemical kinetics dominated the auto-ignition process. Fluid dynamical effects associated with injection phenomena such as spray break and evaporation can be ignored under these circumstances.

Temperature sweeps of the neat oxygenates were performed in the modified IQT at a pressure of 10 bar. This specific pressure was selected because it was required to obtain ignition delay times in excess of aforementioned 40 ms, while still being representative of the end-gas pressure for SI engine operation. Accordingly, we assume SI engine-like pseudo-homogeneous mixtures exist for most of the data.

The IQT chamber was pressurized with air (21% O_2 in N_2) and heated to the highest temperature in the sweep (e.g., 980 K). For lower temperatures, down to 700 K, the heaters were turned off while fuel was injected at regular intervals as the chamber cooled down. To produce an equivalence ratio of 1 at 900 K, the mass of injected fuel was adjusted to accommodate the distinct densities and molecular formulas of the various fuels by using the variable volume injection pump. The volume of the fuel injected can be changed by using metal shims with different thickness, which will change the relative position of the fuel plunger of the in-

jection pump (more detailed description of how to choose the shim thickness are in Appendix A). The mass of fuel injected was then held constant for each temperature sweep, and consequently the equivalence ratio of the combustion events decreased as the combustion chamber cooled. Other studies comparing constant mass to constant equivalence ratio temperature sweeps have shown that the effects of this change in equivalence ratio on ID measurements are small [64–66].

4. Results & discussion

4.1. Engine experiments

4.1.1. Knock intensity and knock limited spark advance

Knock intensity, expressed here as MAPO, increases for all fuels with advancing spark timing (Figure 4). As might be expected from the ON and DCN data presented earlier (Table 5 and 6), the toluene blend shows the greatest knock resistance by allowing the most spark advance before reaching KLSA, with the (alkylated) anisoles trailing close behind (Figure 4). The (alkylated) guaiacols blends, which have ON similar to the base fuel, are more reactive fuels compared to anisoles and toluene, as indicated by the less amounts of possible spark advance. These effects are quantified in Table 8. Evidently, the benzene ring imparts low reactivity to all the oxygenated compounds. Nevertheless, the type and number of functional groups, exert a strong influence on the anti-knock quality.

Based on the RON, MON and the KLSA of the blends, the OI equation (Equation (1)) gives K=-1.28 for this engine at this working condition. This is consistent with results from literature [2, 7], and indicating that fuels with high octane sensitivity are preferred.

Table 8: Knock limited spark advance for all fuels at WOT and 1500 RPM[a]

Fuel	KLSA	KLIMEP	KLEfficiency	KLFuel consumption
	CA bTDC	bar	%	ml/kWh
Euro 95	10.5	14.1	37.3	311.2
10% Toluene	13.9	14.4	38.3	297.8
10% Anisole	12.7	14.3	38.1	303.3
10% 4-MA	13.1	14.3	38.1	301.1
10% 4-PA	13	14.3	37.0	308.7
10% Guaiacol	11.3	14.1	36.9	312.5
10% 4-MG	10.9	14.2	36.9	312.7
10% 4-EG	11.5	14.1	36.5	316.6

[a] All values in this table are taken at the knock limited (KL) spark timing

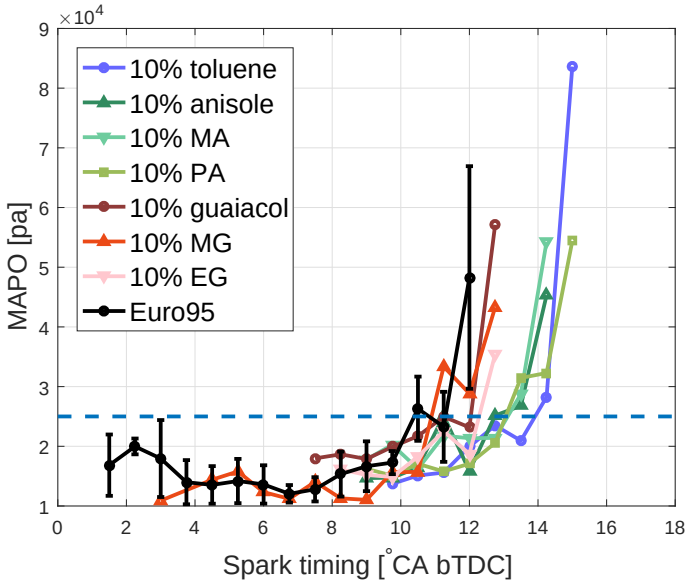

Figure 4: MAPO for all fuels at WOT and 1500 RPM, the dashed line represents the threshold for knock

4.1.2. Efficiency

It can be seen from Figure 5 that when advancing the spark timing, the IMEP is increasing for all the fuels. Fuels with better anti-knock quality allow more advanced spark timings, and thus can achieve higher IMEP. While none of them reached the maximum IMEP due to the knock limitation. This again indicates the importance of having a high anti-knock quality fuel.

More advanced KLSA yields dividends in terms of the engine performance, i.e., IMEP, efficiency and fuel consumption. Among these parameters, fuel conversion efficiency is calculated by Equation 2, where P is power, m is the mass of fuel inducted per cycle.

$$\eta_f = \frac{P}{LHV \times m} \tag{2}$$

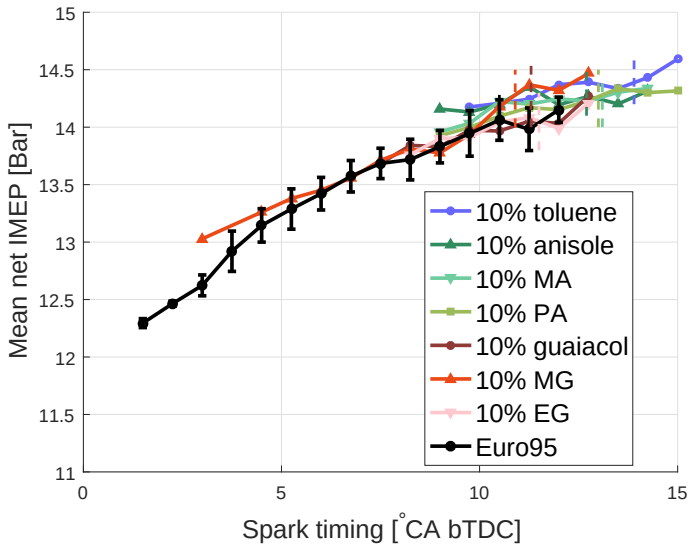

Figure 5: Net IMEP as a function of spark timing for all fuels at WOT and 1500 RPM. Fuel specific KLSA is indicated by dashed bars in the same color

However, The 4-PA and guaiacols blends show a penalty in efficiency relative to the base fuel, a slightly more favorable KLSA (Figure 6) notwithstanding. However, the day-to-day variance has a similar discrepancy to the efficiency difference, therefore, based on our tests, the blends composition has a negligible impact on fuel efficiency.

4.1.3. Fuel consumption

As is true by definition for any oxygenated fuel, the presence of oxygen in the molecular structure has a negative impact on the gravimetric fuel consumption (Figure 7). Notably the guaiacols, having two functional oxygen groups, perform poorly by this measure.

In practice, however, consumers do not pay for mass, they pay for volume and aromatics have high densities relative to gasoline (Table 5). Moreover, as density

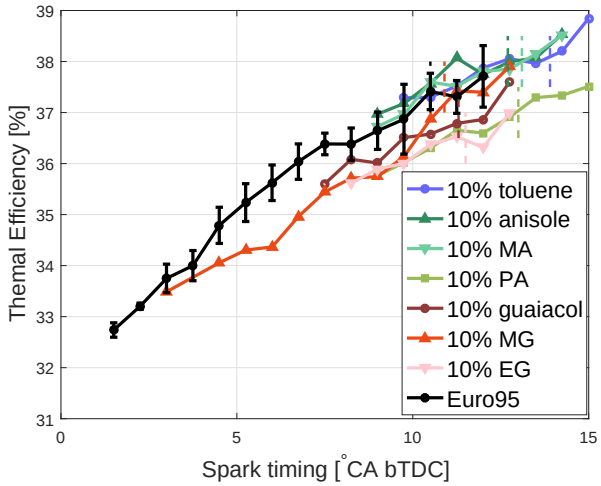

Figure 6: Fuel conversion efficiency as a function of spark timing for all fuels at WOT and 1500 RPM. Fuel specific KLSA is indicated by dashed bars in the same color

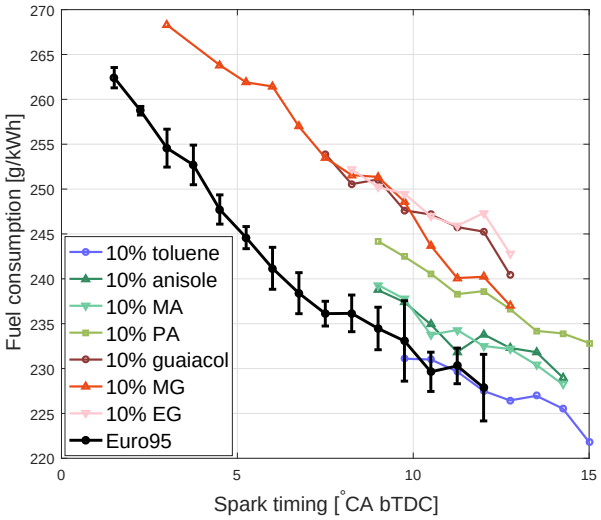

Figure 7: Indicated specific *gravimetric* fuel consumption as a function of spark timing for all fuels at WOT and 1500 RPM. Fuel specific KLSA is indicated by dashed bars in the same color

rises with degree of oxygenation, the spread in volumetric fuel economy is far less pronounced (Figure 8). In fact, the (alkylated) anisole blends yield better fuel consumption than gasoline.

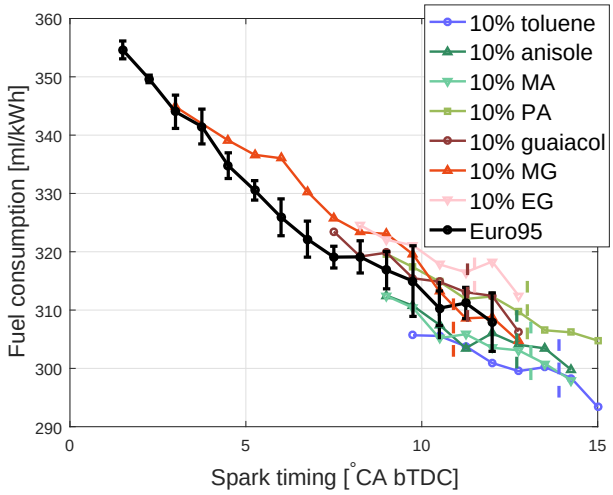

Figure 8: Indicated specific *volumetric* fuel consumption as a function of spark timing for all fuels at WOT and 1500 RPM. Fuel specific KLSA is indicated by dashed bars in the same color

4.2. Constant volume autoignition experiments

Auto-ignition chemistry is quite important for SI engines, since knock is caused by the auto-ignition of the end-gas in the chamber. Therefore, constant volume auto-igniton experiments were conducted for all the oxygenates and toluene.

The temperature dependent autoignition behavior for all studied aromatics at 10 bar, 720-950 K is shown in Figure 9, with iso-octane as a comparison, which has same RON and MON of 100 [64]. As discussed earlier, when the ID is in excess of 40 ms, the ignition process can be assumed to be controlled primarily by chemical kinetics, as opposed to spray physics.

The first thing to note from Figure 9 is that none of these aromatics exhibited any low temperature heat release (LTHR) or negative temperature coefficient (NTC) behavior, in contrast to iso-octane. Analysis of the pressure traces for these compunds confirms the absence of low temperature heat release (Figure 10), therefore the use of the conventional ASTM D6890 definition for start of ignition (i.e., a fixed 138 kPa above the chamber pressure recovery point) is valid [66].

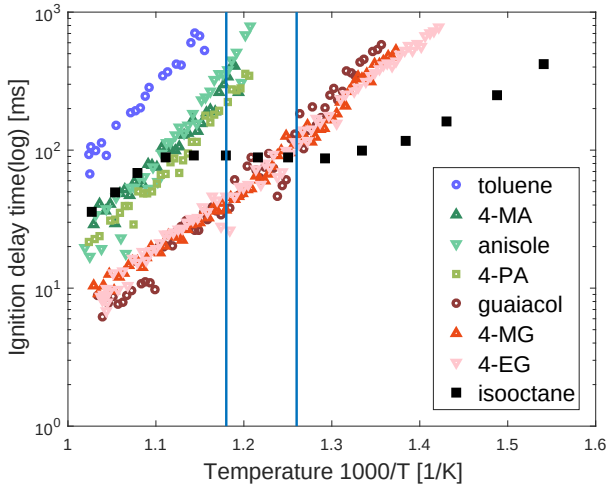

Figure 9: IQT data for all neat aromatics at 10 bar, with iso-octane as a reference from Bogin et al. [64]. The two vertical lines represent the DCN test temperature (818.13±30 K) [62], although, the DCN test pressure is set at 21.4 bar, which is much higher than our test condition.

It can be seen that as expected from the DCN and RON data, toluene has the longest IDs over the entire temperature range studied. Anisole and 4-MA have similar reactivity, however the longer alkyl chain of 4-PA appears to slightly increase its reactivity. The increase in reactivity is stronger upon adding another oxygen functional group to the benzene ring. Guaiacol and its alkylated derivatives have the shortest ID. Note that data from T>800 K can not be assumed as

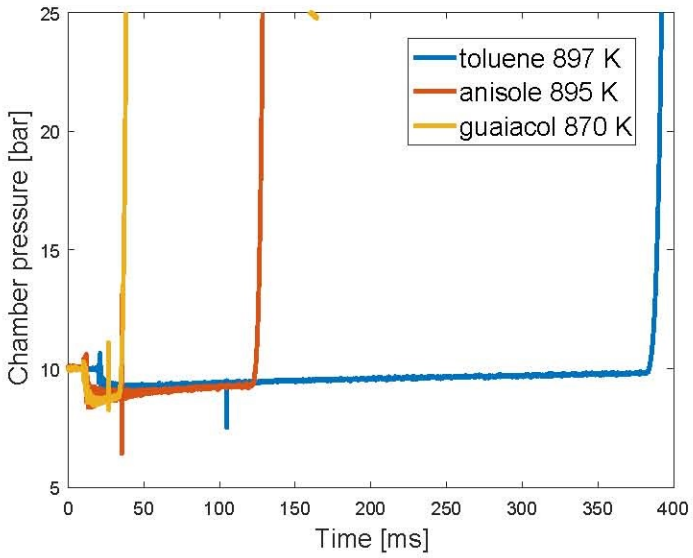

Figure 10: Pressure trace of toluene, anisole and guaiacol at specific temperature in modified IQT at 10 bar

homogeneous auto-ignition for guaiacols

All aromatics are clustered and ranked in accordance with number of functional oxygen groups, irrespective of degree of alkylation (Figure 9).

A fuel's octane number is a measure of its anti-knock rating, and this parameter is dominated by auto-ignition chemistry at the ON test conditions. Badra et al. found that 850 K and 50 atm has the best fit with the RON operating conditions. For MON, this is 980 K and 45 atm [67]. Mehl et al. predicted the ON by using detailed chemistry and a simplified two-zone SI engine model [68].

The IDs for iso-octane, as shown in Figure 9 can also show us some qualitative comparison of ON and this IQT test condition. The auto-igniton of iso-octane is faster than toluene for the whole test range, and it is similar to anisole when T>900 K, from which point on, anisoles yield longer IDs. Compared to iso-

octane, guaiacol is slower when T<800 K, but becomes faster when temperature increases above 800 K. According to the blending RON and MON of anisole and guaiacol, it is expected that anisole will have a higher RON than Euro95, while guaiacol has a RON similar to Euro95, which is slightly lower than the iso-octane data. The left vertical line, which is the upper limit of the DCN temperature requirement, fits for the RON indication. Bogin et al. also found that the ID at higher temperature was more representative of MON conditions [66]. However, more experiments are needed to study this topic further.

5. Conclusions

The goal of this paper was to determine both qualitatively and quantitatively the anti-knock quality of various members of two important families of aromatic oxygenates - anisoles and guaiacols - that are frequent subjects of discussion in lignin related literature. Benchmarked against toluene, the anti-knock quality of these compounds has been evaluated in a port-fuel injected turbo-charged SI engine and a constant volume autoignition experiment. Based on the results of this study, several conclusions may be drawn:

5.1. Fuel properties

- Addition of 10 vol.-% anisole increases the octane number of the RON95 base fuel, but is not as effective as toluene at an equal blend ratio.
- Addition of 10 vol.-% guaiacol has a negligible impact on the octane number of the RON95 base fuel.
- Alkylation of either anisole or guaiacol leads to a modest reduction in RON.

- Gravimetric heating values of the aromatic oxygenates blends are modestly lower than for the RON 95 base fuel.

- Owing to a higher density, volumetric heating values of the aromatic oxygenates blends are modestly higher than for the RON 95 base fuel.

5.2. Engine experiments

- All oxygenated blends made it possible to operate the engine with an earlier knock limited spark advance (KLSA)

- No significant differences in thermal efficiency were observed amongst the tested fuels.

- Modest improvements in volumetric fuel economy were observed for the anisole blends.

- Slight penalties in volumetric fuel economy were measured for the guaiacol blends.

- In general, functionalization by means of oxygenation and to a lesser extent alkylation has a negative impact on anti-knock quality and, by proxy, overall engine performance.

5.3. Constant volume autoignition experiments

- Ignition delay (ID) trends amongst the fuels are in-line with both RON and KLSA data, with the least reactive fuels consistently yielding the longest ID.

- Alkylation generally has a modest impact on ID, with the exception of long side chains at low temperature. In all cases, alkylation leads to a shorter ID.
- Oxygenation has a strong impact on ID, with the ID becoming shorter and shorter as more functional oxygen groups are added to the ring.

In short, the anti-knock quality of aromatic oxygenates suffers from functionalization, whereby oxygenation appears to be far more detrimental than alkylation. Lignin conversion stakeholders should take this into account in their cost-benefit analysis.

Acknowledgments

The authors would like to thank Lisa Fouts, Earl Christensen from the National Renewable Energy Laboratory for their help with the experimental work. Financial support for the National Renewable Energy Laboratory employees was provided by the U.S. Department of Energy - Vehicles Technologies Office, under Contract No. DE347AC36-99GO10337 with the National Renewable Energy Laboratory. The authors also gratefully acknowledge SER-Brabant (New Energy House project) and the Chinese Scholarship Council (CSC) for their financial support and, finally, Volvo Car Corporation for technical support regarding the engine tests.

References

[1] T. G. Leone, J. E. Anderson, R. S. Davis, A. Iqbal, R. A. Reese, M. H. Shelby, et al., The effect of compression ratio, fuel octane rating, and ethanol

content on spark-ignition engine efficiency, Environ. Sci. Technol. 49 (18) (2015) 10778–89. doi:10.1021/acs.est.5b01420.

[2] G. Kalghatgi, Fuel Anti-Knock Quality - Part I. Engine Studies, SAE Tech. Pap. 2001-01-3584. doi:10.4271/2001-01-3584.

[3] G. Kalghatgi, Fuel anti-knock quality- Part II. Vehicle studies - how relevant is motor Octane Number (MON) in modern engines?, SAE Tech. Pap. 2001-01-3585. doi:10.4271/2001-01-3585.

[4] G. Kalghatgi, Auto-ignition quality of practical fuels and implications for fuel requirements of future si and hcci engines, SAE Tech. Pap. 2005-01-0239. doi:10.4271/2005-01-0239.

[5] V. Mittal, J. B. Heywood, The shift in relevance of fuel RON and MON to knock onset in modern SI engines over the last 70 years, SAE Int. J. Engines 2 (2009) 2009–01–2622. doi:10.4271/2009-01-2622.

[6] Council of European Union, Directive 2009/30/ec of the european parliament and of the council (2009).

[7] A. Amer, H. Babiker, J. Chang, G. Kalghatgi, P. Adomeit, A. Brassat, et al., Fuel effects on knock in a highly boosted direct injection spark ignition engine, SAE Int. J. Fuels Lubr. 5 (3) (2012) 2012–01–1634. doi:10.4271/2012-01-1634.

[8] Platts, [accessed 01.05.2016], http://www.platts.com/latest-news/petrochemicals/london/nwe-ethyl-tert-butyl-ether-at-lowest-spot-price-26236377.

[9] M. Tian, R. Van Haaren, J. Reijnders, M. Boot, Lignin derivatives as potential octane boosters, SAE Int. J. Fuels Lubr. 8 (2) (2015) 415–422. doi:10.4271/2015-01-0963.

[10] R. L. McCormick, M. A. Ratcliff, E. Christensen, L. Fouts, J. Luecke, G. M. Chupka, et al., Properties of oxygenates found in upgraded biomass pyrolysis oil as components of spark and compression ignition engine fuels, Energy Fuels 29 (2015) 2453–61. doi:10.1021/ef502893g.

[11] V. S. B. Shankar, M. Al-Abbad, M. El-Rachidi, S. Y. Mohamed, E. Singh, Z. Wang, et al., Antiknock quality and ignition kinetics of 2-phenylethanol, a novel lignocellulosic octane booster, Proc. Combust. Inst. 000 (2016) 1–8. doi:10.1016/j.proci.2016.05.041.

[12] L. Zhou, M. D. Boot, L. P. H. de Goey, The effect of the position of oxygen group to the aromatic ring to emission performance in a heavy-duty diesel engine, SAE Int. J. Fuels Lubr. 5 (3) (2012) 2012–01–1697. doi:10.4271/2012-01-1697.

[13] L. Zhou, M. Boot, B. Johansson, J. Reijnders, Performance of lignin derived aromatic oxygenates in a heavy-duty diesel engine, Fuel 115 (2014) 469–478. doi:10.1016/j.fuel.2013.07.047.

[14] M. E. Baumgardner, T. L. Vaughn, A. Lakshminarayanan, D. Olsen, M. A. Ratcliff, R. L. McCormick, et al., Combustion of lignocellulosic biomass based oxygenated components in a compression ignition engine, Energy Fuels 29 (11) (2015) 7317–26. doi:10.1021/acs.energyfuels.5b01595.

[15] J. Herreros, A. Jones, E. Sukjit, A. Tsolakis, Blending lignin-derived oxygenate in enhanced multi-component diesel fuel for improved emissions, Appl. Energy 116 (2014) 58–65. doi:10.1016/j.apenergy.2013.11.022.

[16] L. Zhou, B. Heuser, M. Boot, F. Kremer, S. Pischinger, Performance and emissions of lignin and cellulose based oxygenated fuels in a compression-ignition engine, SAE Tech. Pap. 2015-01-09. doi:10.4271/2015-01-0910.

[17] L. Zhou, M. Boot, B. Johansson, Comparison of emissions and performance between saturated cyclic oxygenates and aromatics in a heavy-duty diesel engine, Fuel 113 (2013) 239–247. doi:10.1016/j.fuel.2013.05.018.

[18] B. Rajesh Kumar, S. Saravanan, R. Niranjan Kumar, B. Nishanth, D. Rana, A. Nagendran, Effect of lignin-derived cyclohexanol on combustion, performance and emissions of a direct-injection agricultural diesel engine under naturally aspirated and exhaust gas recirculation (EGR) modes, Fuel 181 (2016) 630–642. doi:10.1016/j.fuel.2016.05.052.

[19] Q. Bu, H. Lei, A. H. Zacher, L. Wang, S. Ren, J. Liang, et al., A review of catalytic hydrodeoxygenation of lignin-derived phenols from biomass pyrolysis., Bioresour. Technol. 124 (2012) 470–7. doi:10.1016/j.biortech.2012.08.089.

[20] F. S.Chakar, A. J.Ragauskas, Review of current and future softwood kraft lignin process chemistry, Ind. Crops Prod. 20 (2004) 131–141. doi:10.1016/j.indcrop.2004.04.016.

[21] G. W. Huber, S. Iborra, A. Corma, Synthesis of transportation fuels from

biomass: chemistry, catalysts, and engineering., Chem. Rev. 106 (2006) 4044–98. doi:10.1021/cr068360d.

[22] A. U. Buranov, G. Mazza, Lignin in straw of herbaceous crops, Ind. Crops Prod. 28 (2008) 237–259. doi:10.1016/j.indcrop.2008.03.008.

[23] T. Prasomsri, T. Nimmanwudipong, Y. Román-Leshkov, Effective hydrodeoxygenation of biomass-derived oxygenates into unsaturated hydrocarbons by MoO_3 using low H_2 pressures, Energy Environ. Sci. 6 (6) (2013) 1732–8. doi:10.1039/c3ee24360e.

[24] T. Prasomsri, M. Shetty, K. Murugappan, Y. Roman-Leshkov, Insights into the catalytic activity and surface modification of moo_3 during the hydrodeoxygenation of lignin-derived model compounds into aromatic hydrocarbons under low hydrogen pressures, Energy Environ. Sci. 7 (2014) 2660–9. doi:10.1039/C4EE00890A.

[25] T. D. H. Nguyen, M. Maschietti, L.-E. Åmand, L. Vamling, L. Olausson, S.-I. Andersson, et al., The effect of temperature on the catalytic conversion of kraft lignin using near-critical water, Bioresour. Technol. 170 (2014) 196–203. doi:10.1016/j.biortech.2014.06.051.

[26] M. Saidi, F. Samimi, D. Karimipourfard, T. Nimmanwudipong, B. C. Gates, M. R. Rahimpour, Upgrading of lignin-derived bio-oils by catalytic hydrodeoxygenation, Energy Environ. Sci. 7 (1) (2014) 103. doi:10.1039/c3ee43081b.

[27] A. L. Jongerius, R. Jastrzebski, P. C. A. Bruijnincx, B. M. Weckhuysen,

CoMo sulfide-catalyzed hydrodeoxygenation of lignin model compounds: An extended reaction network for the conversion of monomeric and dimeric substrates, J. Catal. 285 (1) (2012) 315–323. doi:10.1016/j.jcat.2011.10.006.

[28] B. P. Mudraboyina, S. Farag, A. Banerjee, J. Chaouki, P. G. Jessop, Supercritical fluid rectification of lignin pyrolysis oil methyl ether (LOME) and its use as a bio-derived aprotic solvent, Green Chem. (2016) 13–6doi:10.1039/C5GC02233A.

[29] M. S. Talmadge, R. M. Baldwin, M. J. Biddy, R. L. McCormick, G. T. Beckham, G. A. Ferguson, et al., A perspective on oxygenated species in the refinery integration of pyrolysis oil, Green Chem. 16 (2014) 407–453. doi:10.1039/C3GC41951G.

[30] K. Okuda, M. Umetsu, S. Takami, T. Adschiri, Disassembly of lignin and chemical recoveryrapid depolymerization of lignin without char formation in waterphenol mixtures, Fuel Process. Technol. 85 (2004) 803–813. doi:10.1016/j.fuproc.2003.11.027.

[31] D. M. Alonso, S. G. Wettstein, J. A. Dumesic, Bimetallic catalysts for upgrading of biomass to fuels and chemicals, Chem. Soc. Rev. 41 (2012) 8075–8098. doi:10.1039/C2CS35188A.

[32] D. A. Ruddy, J. A. Schaidle, J. R. Ferrell III, J. Wang, L. Moens, J. E. Hensley, Recent advances in heterogeneous catalysts for bio-oil upgrading via ”ex situ catalytic fast pyrolysis”: catalyst development through the study of model compounds, Green Chem. 16 (2014) 454–490. doi:10.1039/C3GC41354C.

[33] N. Joshi, A. Lawal, Hydrodeoxygenation of 4-propylguaiacol (2-methoxy-4-propylphenol) in a microreactor: Performance and kinetic studies, Ind. Eng. Chem. Res. 52 (11) (2013) 4049–4058. doi:10.1021/ie400037y.

[34] X. Bai, K. H. Kim, R. C. Brown, E. Dalluge, C. Hutchinson, Y. J. Lee, et al., Formation of phenolic oligomers during fast pyrolysis of lignin, Fuel 128 (2014) 170–9. doi:10.1016/j.fuel.2014.03.013.

[35] X.-F. Zhou, Conversion of kraft lignin under hydrothermal conditions, Bioresour. Technol. 170 (2014) 583–6. doi:10.1016/j.fuel.2013.07.047.

[36] E. Taarning, C. M. Osmundsen, X. Yang, B. Voss, S. I. Andersen, C. H. Christensen, Zeolite-catalyzed biomass conversion to fuels and chemicals, Energy Environ. Sci. 4 (2011) 793–804. doi:10.1039/C004518G.

[37] C. Font Palma, Modelling of tar formation and evolution for biomass gasification: A review, Appl. Energy 111 (2013) 129–141. doi:10.1016/j.apenergy.2013.04.082.

[38] X. Wang, R. Rinaldi, Exploiting H-transfer reactions with RANEY®Ni for upgrade of phenolic and aromatic biorefinery feeds under unusual, low-severity conditions, Energy Environ. Sci. 5 (2012) 8244–8260. doi:10.1039/C2EE21855K.

[39] A. L. Jongerius, P. C. A. Bruijnincx, B. M. Weckhuysen, Liquid-phase reforming and hydrodeoxygenation as a two-step route to aromatics from lignin, Green Chem. 15 (11) (2013) 3049–56. doi:10.1039/c3gc41150h.

[40] A. Vigneault, D. K. Johnson, E. Chornet, Base-catalyzed depolymerization of lignin: separation of monomers, Can. J. Chem. Eng. 85 (2007) 906–916. doi:10.1002/cjce.5450850612.

[41] R. Olcese, M. Bettahar, D. Petitjean, B. Malaman, F. Giovanella, A. Dufour, Gas-phase hydrodeoxygenation of guaiacol over Fe/SiO_2 catalyst, Appl. Catal. B Environ. 115-116 (2012) 63–73. doi:10.1016/j.apcatb.2011.12.005.

[42] H. Pikowska, P. Wolak, A. Zociska, Hydrothermal decomposition of alkali lignin in sub- and supercritical water, Chem. Eng. J. 187 (2012) 410–4. doi:10.1016/j.cej.2012.01.092.

[43] X. Huang, T. I. Korányi, M. D. Boot, E. J. M. Hensen, Catalytic depolymerization of lignin in supercritical ethanol, ChemSusChem 7 (2014) 2276–2288. doi:10.1002/cssc.201402094.

[44] Y. Ye, Y. Zhang, J. Fan, J. Chang, Novel method for production of phenolics by combining lignin extraction with lignin depolymerization in aqueous ethanol, Ind. Eng. Chem. Res. 51 (1) (2012) 103–110. doi:10.1021/ie202118d.

[45] X. Ma, R. Ma, W. Hao, M. Chen, F. Yan, K. Cui, et al., Common pathways in ethanolysis of kraft lignin to platform chemicals over molybdenum-based catalysts, ACS Catalysis 5 (8) (2015) 4803–13. doi:10.1021/acscatal.5b01159.

[46] C. Xu, R. A. D. Arancon, J. Labidi, R. Luque, Lignin depolymerisation

strategies: towards valuable chemicals and fuels, Chem. Soc. Rev. 43 (2014) 7485–7500. doi:10.1039/C4CS00235K.

[47] C. Liu, H. Wang, A. M. Karim, J. Sun, Y. Wang, Catalytic fast pyrolysis of lignocellulosic biomass, Chem. Soc. Rev. 43 (2014) 7594–7623. doi:10.1039/C3CS60414D.

[48] S. I. Yang, M. S. Wu, C. Y. Wu, Application of biomass fast pyrolysis part I: Pyrolysis characteristics and products, Energy 66 (2014) 162–171. doi:10.1016/j.energy.2013.12.063.

[49] A. Brandt, L. Chen, B. E. van Dongen, T. Welton, J. P. Hallett, Structural changes in lignins isolated using an acidic ionic liquid water mixture, Green Chem. 17 (2015) 5019–5034. doi:10.1039/C5GC01314C.

[50] R. J. A. Gosselink, W. Teunissen, J. E. G. van Dam, E. de Jong, G. Gellerstedt, E. L. Scott, et al., Lignin depolymerisation in supercritical carbon dioxide/acetone/water fluid for the production of aromatic chemicals., Bioresour. Technol. 106 (2012) 173–7. doi:10.1016/j.biortech.2011.11.121.

[51] D. Fu, S. Farag, J. Chaouki, P. G. Jessop, Extraction of phenols from lignin microwave-pyrolysis oil using a switchable hydrophilicity solvent, Bioresour. Technol. 154 (2014) 101–8. doi:10.1016/j.biortech.2013.11.091.

[52] O. D. Mante, J. A. Rodriguez, S. P. Babu, Selective defunctionalization by TiO_2 of monomeric phenolics from lignin pyrolysis into simple phenols, Bioresour. Technol. 148 (2013) 508–516. doi:10.1016/j.biortech.2013.09.003.

[53] X. Huang, T. I. Koranyi, M. D. Boot, E. J. M. Hensen, Ethanol as capping agent and formaldehyde scavenger for efficient depolymerization of lignin to aromatics, Green Chem. 17 (2015) 4941–4950. doi:10.1039/C5GC01120E.

[54] C. Zhao, J. A. Lercher, Selective hydrodeoxygenation of lignin-derived phenolic monomers and dimers to cycloalkanes on Pd/C and HZSM-5 catalysts, ChemCatChem 4 (2012) 64–68. doi:10.1002/cctc.201100273.

[55] Q. Song, F. Wang, J. Cai, Y. Wang, J. Zhang, W. Yu, et al., Lignin depolymerization (ldp) in alcohol over nickel-based catalysts via a fragmentation-hydrogenolysis process, Energy Environ. Sci. 6 (2013) 994–1007. doi:10.1039/C2EE23741E.

[56] R. Lou, S. B. Wu, Products properties from fast pyrolysis of enzymatic/mild acidolysis lignin, Appl. Energy 88 (1) (2011) 316–322. doi:10.1016/j.apenergy.2010.06.028.

[57] Standard test method for determination of individual components in spark ignition engine fuels by 100 metre capillary high resolution gas chromatography, ASTM D6729-14.

[58] J. Yanowitz, M. A. Ratcliff, R. McCormick, J. Taylor, M. Murphy, Compendium of experimental cetane number data, Tech. Rep. NREL/TP-5400-61693, National Renewable Energy Laboratory (2004).

[59] V. Knop, M. Loos, C. Pera, N. Jeuland, A linear-by-mole blending rule for octane numbers of n-heptane/iso-octane/ toluene mixtures, Fuel 115 (2014) 666–673. doi:10.1016/j.fuel.2013.07.093.

[60] B. Zhmud, Viscosity blending equations, Lube magazine (121) (2014) 24–29.

[61] X. Zhen, Y. Wang, S. Xu, Y. Zhu, C. Tao, T. Xu, et al., The engine knock analysis An overview, Appl. Energy 92 (2012) 628–636. doi:10.1016/j.apenergy.2011.11.079.

[62] Standard test method for determination of ignition delay and derived cetane number (DCN) of diesel fuel oils by combustion in a constant volume chamber, ASTM D6890-03a.

[63] G. E. Bogin, A. DeFilippo, J. Y. Chen, G. Chin, J. Luecke, M. A. Ratcliff, et al., Numerical and experimental investigation of n-heptane autoignition in the ignition quality tester (IQT), Energy Fuels 25 (2011) 5562–72. doi:10.1021/ef201079g.

[64] G. E. Bogin, E. Osecky, M. A. Ratcliff, J. Luecke, X. He, B. T. Zigler, et al., Ignition quality tester (IQT) investigation of the negative temperature coefficient region of alkane autoignition, Energy Fuels 27 (2013) 1632–42. doi:10.1021/ef301738b.

[65] G. E. Bogin, E. Osecky, J. Y. Chen, M. A. Ratcli, J. Luecke, B. T. Zigler, et al., Experiments and computational fluid dynamics modeling analysis of large n-alkane ignition kinetics in the ignition quality tester, Energy Fuels 27 (7) (2014) 4781–94. doi:10.1021/ef500769j.

[66] G. E. Bogin, J. Luecke, M. A. Ratcliff, E. Osecky, B. T. Zigler, Effects of iso-octane/ethanol blend ratios on the observance of negative temperature

coefficient behavior within the Ignition Quality Tester, Fuel 186 (2016) 82–90. doi:10.1016/j.fuel.2016.08.021.

[67] J. A. Badra, N. Bokhumseen, N. Mulla, S. M. Sarathy, A. Farooq, G. Kalghatgi, P. Gaillard, A methodology to relate octane numbers of binary and ternary n-heptane, iso-octane and toluene mixtures with simulated ignition delay times, Fuel 160 (2015) 458–469. doi:10.1016/j.fuel.2015.08.007.

[68] M. Mehl, T. Faravelli, F. Giavazzi, E. Ranzi, P. Scorletti, A. Tardani, et al., Detailed chemistry promotes understanding of octane numbers and gasoline sensitivity, Energy Fuels 20 (6) (2006) 2391–2398. doi:10.1021/ef060339s.

Appendices

A. Appendix A

Gravimetric fuel consumption is calculated by using the measured mole count of air in the combustion vessel at a given pressure and temperature. First, this data is used to calculate how much fuel is required for the stoichiometric case. Subsequently, the shim thickness, which is related to the amount of the injected fuel, is calculated by using linear calibration of the injected amount of fuel and the required shim thickness in the fuel injection pump. The amount of fuel injected is controlled using the method outlined in the IQT operating manual.

Viscosity is an important parameter for injection at room temperature and atmospheric conditions. Three reference fuels, n-heptane, decane and hexadecane,

each having a distinct viscosity, were tested in order to derive a correlation between shim thickness and the injected fuel mass. Figure 11 shows the calibration results of this relationship.

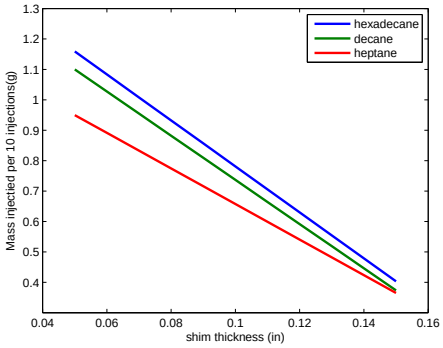

Figure 11: Calibration of injected mass for various model fuels

The viscosity of hexadecane at $3 \times 10^{-3} Pa \cdot s$ is roughly half that of guaiacol. Nevertheless, it is the best proxy for guaiacol amongst the reference fuels, so its data is used for calculating the shim thickness for the guaiacols.

Anisole and toluene have a viscosity of $1 \times 10^{-3} Pa \cdot s$ and $0.56 \times 10^{-3} Pa \cdot s$, respectively. Both values are close to that of decane ($0.93 \times 10^{-3} Pa \cdot s$). Decane data is therefore used to calculate the shim thickness for the anisoles (and toluene).

The figure shows that, as the shim becomes thicker, the differences between the different fuels become smaller. For the aromatic fuels considered in this study, the shim is always $> 0.09 in$, which means the impact of viscosity is not significant here.